



Universidad
Zaragoza

Trabajo Fin de Máster

Influencia de la rigidez de la matriz extracelular en
la migración celular en tres dimensiones

The role of the matrix stiffness on 3D cell migration

Autor

Francisco Serrano Alcalde

Directores

José Manuel García Aznar
Ismael D. González Valverde

ESCUELA DE INGENIERÍA Y ARQUITECTURA

2017

DECLARACIÓN DE
AUTORÍA Y ORIGINALIDAD

(Este documento debe acompañar al Trabajo Fin de Grado (TFG)/Trabajo Fin de Máster (TFM) cuando sea depositado para su evaluación).

D./D^a. Francisco Serrano Alcalde,

con nº de DNI 73092087-L en aplicación de lo dispuesto en el art.

14 (Derechos de autor) del Acuerdo de 11 de septiembre de 2014, del Consejo

de Gobierno, por el que se aprueba el Reglamento de los TFG y TFM de la

Universidad de Zaragoza,

Declaro que el presente Trabajo de Fin de (Grado/Máster)
Máster _____, (Título del Trabajo)

Influencia de la rigidez de la matriz extracelular en la migración celular en tres
dimensiones

es de mi autoría y es original, no habiéndose utilizado fuente sin ser citada
debidamente.

Zaragoza, 22 de Junio de 2017

Fdo: Francisco Serrano Alcalde

All things are difficult before they are easy.
Thomas Fuller

Agradecimientos

En primer lugar, me gustaría comenzar dando las gracias a los directores de este Trabajo Fin de Máster por su apoyo durante todo este tiempo. Por sacar siempre un hueco para resolver las dudas que han ido surgiendo y por confiar en mí desde el primer día. Me habéis mostrado el maravilloso, aunque por momentos frustrante, mundo de la investigación. Por todo ello, gracias.

También quiero agradecer a mis padres, hermano, tíos, primos y abuelos por el apoyo incondicional que siempre me habéis dado y haber sido una motivación constante. Gracias.

A Irene, por acompañarme y entenderme durante todo este tiempo.

Por último, este trabajo ha sido financiado por el Consejo Europeo de Investigación (ERC) a través del Proyecto ERC-2012-StG 306751 y el Ministerio Español de Economía y Competitividad a través del Proyecto DPI2015-64221-C2-1-R. Este trabajo ha sido parcialmente financiado por la Unión European (a través de los Fondos Europeos de Desarrollo Regional).

Resumen

Influencia de la rigidez de la matriz extracelular en la migración celular en tres dimensiones

En el presente Trabajo Fin de Máster se pretende estudiar uno de los tipos de migración celular conocidos del que todavía no se entiende con certeza qué condiciones deben darse para que se produzca, migración basada en lobopodia.

Para la ingeniería de tejidos, así como enfermedades en las que entender los procesos de migración celular tiene un papel fundamental, resulta necesario realizar estudios tanto experimentales como computacionales para avanzar en su conocimiento. Hasta ahora la mayoría de estudios se han realizado en dos dimensiones (2D), sin embargo, con el avance de la tecnología y la posibilidad de realizar ensayos en tres dimensiones (3D) se ha descubierto un nuevo tipo de migración celular, migración basada en lobopodia.

Este tipo de migración sólo aparece en matrices extracelulares 3D, aunque sólo bajo ciertas condiciones que todavía no están claras. En ella, la célula crea una protusión a través de la cual el núcleo comienza a pasar y actúa de pistón, dividiendo la célula en dos partes y aumentando la presión en la parte delantera.

Una de las hipótesis existentes sobre cuándo aparece este tipo de migración es que depende de las propiedades mecánicas de la matriz extracelular. Según si ésta es elástica lineal o elástica no lineal (además de otros factores químicos) aparecerá el lobopodio y el núcleo comenzará a pasar a través de él.

Para intentar dilucidar si las propiedades mecánicas de la matriz tienen influencia o no en la elección del tipo de migración, se ha desarrollado un modelo de elementos finitos partiendo de un ensayo realizado en el laboratorio del M2BE, en el cual una célula de fibroblasto migra usando lobopodia, para simular distintas matrices con diferentes propiedades mecánicas (rigidez, compresibilidad, elástica lineal o dependiente de la deformación).

Abstract

The role of the matrix stiffness on 3D cell migration

In this Master's Thesis, we study a cellular migration type that is known as lobopodia-based migration. The conditions under which this type of migration occurs is at least unknown.

For tissue engineering, just like human diseases in which understanding the cellular migration processes plays a fundamental role, it is necessary to carry out experimental and computational studies to progress in their knowledge. Until now, the most of studies have been made in two dimensions (2D), however, with the advance of technology and the possibility to make tests in three dimensions (3D), it has been discovered a new type of cellular migration, lobopodia-based migration.

This type of migration only appears in extracellular matrices 3D, although only under certain conditions which are not yet clear. In lobopodia-based migration, the cell creates a protrusion through which the nucleus begins to pass and acts as a piston, dividing the cell in two parts and increasing the pressure in the front part.

One of the existing hypotheses about when this type of migration appears is that it depends on the mechanical properties of the extracellular matrix. Depending on whether it is linear elastic or non-linear elastic, the lobopodio will appear and the nucleus will begin to move (in addition to other chemical factors).

In order to elucidate if the mechanical properties of the extracellular matrix are crucial in the choice of cell migration, we propose here a finite element model in which we simulate a test lab for different matrices with different mechanical properties and behaviours (stiffness, compressibility, linear elastic or strain-dependent) for a single cell migration using lobopodia-based.

Contents

1	Introduction	1
2	Materials and Methods	4
2.1	Geometry and FE discretization	4
2.2	Materials	6
2.3	Boundary and loading conditions	9
3	Results and discussion	11
3.1	Nucleus displacement through lobopodio	11
3.2	Hydrostatic pressure in the cytoplasm	13
3.3	Strains of the matrix	14
3.4	Nucleus stress	17
4	Conclusion	21
4.1	Future work	23
	Bibliography	24
A	Porous elastic material	27
B	Computational model of rheometer	30

Chapter 1

Introduction

In recent years, several studies have investigated the mechanical properties of the extracellular matrix (ECM) and the mechanisms of cellular migration [1, 2, 3]. Understanding how and why cells are able to sense the ECM stiffness and select the best migration strategy have become crucial to progress in other areas, such as, tissue engineering, cancer progression or injury regeneration.

Cell migration on two dimensions (2D) has been extensively described on previous experimental works. These studies have revealed some basic migration mechanisms, such as lamellipodia, adhesion-mediated traction or actomyosin contractility [4]. There are different studies relating the mode of cell migration with the mechanical properties of the ECM [2, 5, 6, 7, 8]. These mechanisms depend on the cell type and their physical environments. To better understand the cellular behaviour, several authors studied the influence of ECM molecular composition [9], the density and orientation of fibrillary elements, the bulk and local stiffness [10] and the mechanical response of the ECM [5].

However, cell movement in the human body mainly occurs on three dimensions (3D). Petrie et al. [5] proposed a new mode of single cell migration, lobopodia-based (Figure 1.1 a), which only takes place in 3D ECMs. The nucleus acts as a piston which polarizes internal pressure and creates protrusions that facilitate cell movement. The pressure in the leading edge is three times bigger in lobopodia-based than in lamellipodia-based migration. On lamellipodia-based migration (Figure 1.1 b), the cell uses different lamellae to move instead of a single large cylindrical protrusion (lobopodia). These experiments have been mainly performed with primary human fibroblasts.

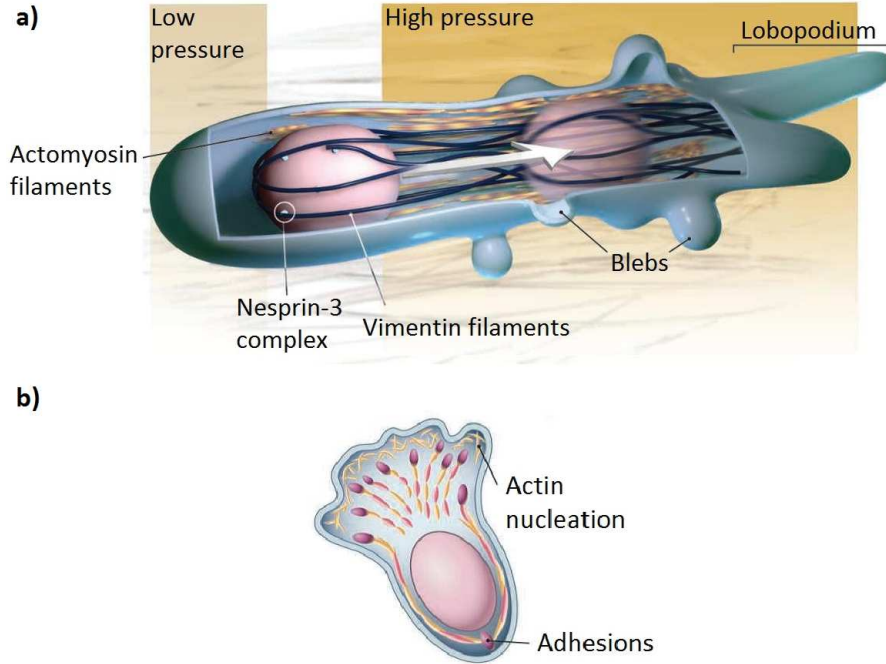


Figure 1.1: Scheme of cell Lobopodio (a) and cell Lamellipodio (b) [6].

Petrie et al. [7] showed that a single fibroblast may switch from actin-driven lamellipodial protrusion to a nuclear piston lobopodial-driven mode of migration. The migration mode depends on the mechanical properties of ECM. To elucidate when and where this kind of migration is used, they carried out a study with different ECMs [5]. Two mechanical parameters were analysed, the elastic or Young's modulus (E) and strain stiffening, a measurement of how the stiffness of a material depends on the strain. They used an atomic force microscope (AFM) to measure the force and the strain applied, after that, they computed the Young's modulus. They obtained E_{med} from this measure and E_{high} from another measurement of Young's modulus with a greater force and deformation. For a linear elastic material the Young's modulus is constant ($E_{high}/E_{med} = 1$), however, a non-linear material presents strain-dependency and the elastic modulus increases with the strain ($E_{high}/E_{med} > 1$).

Their main conclusion is that the mechanical response of the ECM is related with the mode of cell migration, but the reason of these differences are still unclear.

The purpose of this Master's Thesis is to elucidate how the mechanical properties of the ECM may affect lobopodial-based migration. To determine the influence of ECM non-linear elastic behaviour, we analyse the nucleus displacement, the gradient of hydrostatic pressure between the front and the back part of the nucleus in the cytoplasm, the stresses in the nucleus and the deformation levels in the ECM in function of its mechanical behaviour.

Chapter 2

Materials and Methods

In this section, it is shown the process followed in order to create Finite Element-based models that allow the three-dimensional (3D) simulations of single cell migration using lobopodia. Initially, it is presented the geometry of the cell and the corresponding discretization. Secondly, the mechanical behaviour of the different materials that define our problem are presented, distinguishing between cell and ECM. Finally, the initial boundary and loading conditions are described.

2.1 Geometry and FE discretization

The initial geometry established for all simulations is a cube with $150 \times 100 \times 100$ (μm) for the extracellular matrix and an axisymmetric section defined in Figure 2.1 for the cell body with the corresponding cytoplasm and nucleus. This geometry was obtained from a video filmed on a cell migration experiment from M2BE lab (Figure 2.2).

Regarding the finite element discretization, the model is simulated using coincident nodes condition to reduce the computational cost and favour the convergence. Table 2.1 shows the number and type of elements used in the model. On the one hand, we use solid mechanics and pore pressure elements for the cytoplasm because we consider it as a solid and fluid two-phase composition. On the other hand, we use solid mechanics hybrid elements for the nucleus in order to get better convergence because of the quasi-incompressibility of the nucleus. Furthermore, a mesh sensitivity study

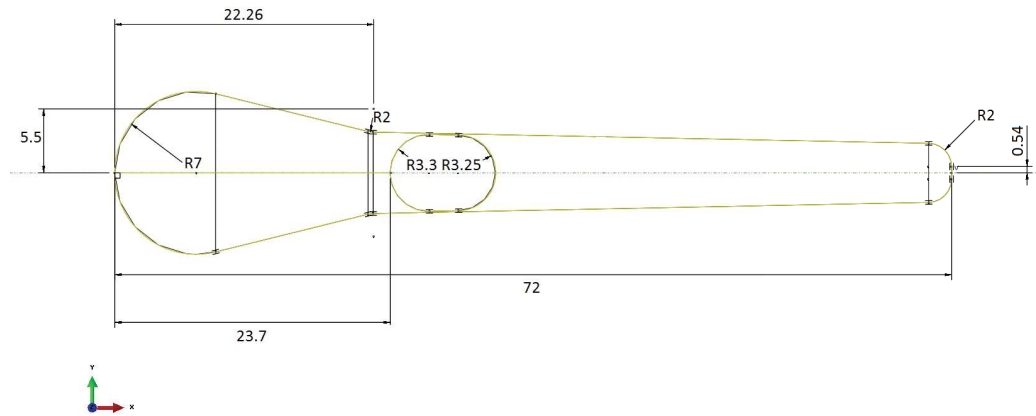


Figure 2.1: Cell section (units μm).

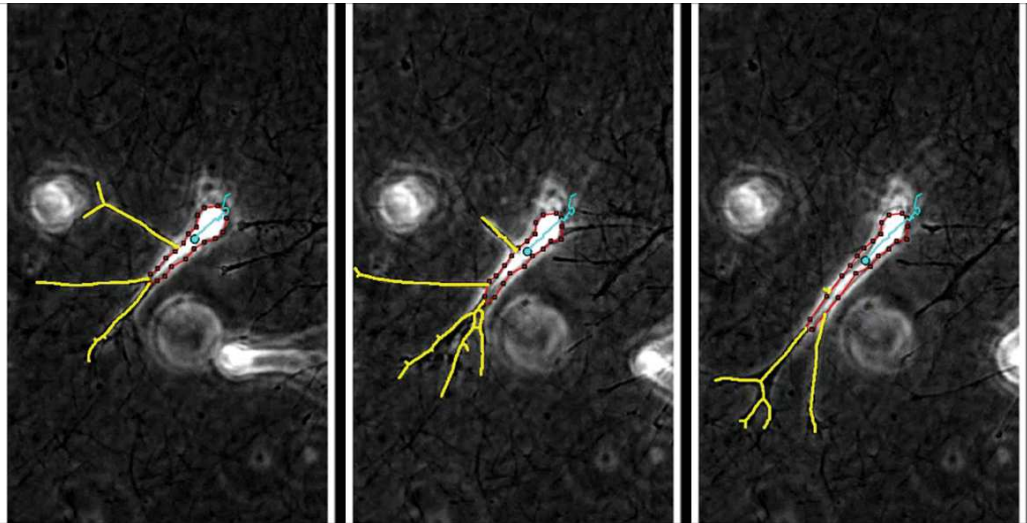


Figure 2.2: Cell in a 2 mg/ml of collagen matrix. Photos taken in a real experiment from M2BE laboratory.

was performed by increasing the total number of elements up to 3.745.614; the results were comparable, but the calculation time significantly increased.

Part	Element type	Number of elements
ECM	631922	Tetrahedral solid mechanics (C3D4)
Cytoplasm	28387	Tetrahedral solid mechanics and pore pressure (C3D4P)
Nucleus	1651	Tetrahedral solid mechanics hybrid (C3D4H)

Table 2.1: Number and type of elements used in the model.

2.2 Materials

We simulate five different matrices (Table 2.2). Three of them with constant Young's modulus: CDM (cell-derived matrix) [5], dermal explant [5] and elastic collagen (a simulation of the 2 *mg/ml* collagen hydrogel without strain-dependent behaviour, Figure 2.3). And the other two with a strain-dependent behaviour: 2 and 4 *mg/ml* collagen hydrogel [11].

Matrix	Initial Young's modulus (Pa)	Strain-dependent
2 <i>mg/ml</i> collagen hydrogel	118	Yes
4 <i>mg/ml</i> collagen hydrogel	340	Yes
Elastic collagen	118	No
CDM	627	No
Dermal explant	6427	No

Table 2.2: Summary of matrix properties.

The matrices CDM and dermal explant are obtained from the work of Petrie et al. [5]. Otherwise, to obtain the equivalent elastic modulus from the 2 *mg/ml* collagen hydrogel, we use the relation between the shear modulus and Young's modulus and Poisson's ratio:

$$G = \frac{E}{2 \cdot (1 + \nu)} \quad (2.1)$$

where G is the shear modulus, E is the Young's modulus and ν the Poisson's ratio. We fix the Poisson's ratio to 0.48 following Petrie et al. [5]. Table 2.3 shows shear stress versus shear strain for a computational shear test

(Appendix B). All linear elastic matrices are modelled as a elastic material defined by the Young's modulus and the Poisson's ratio.

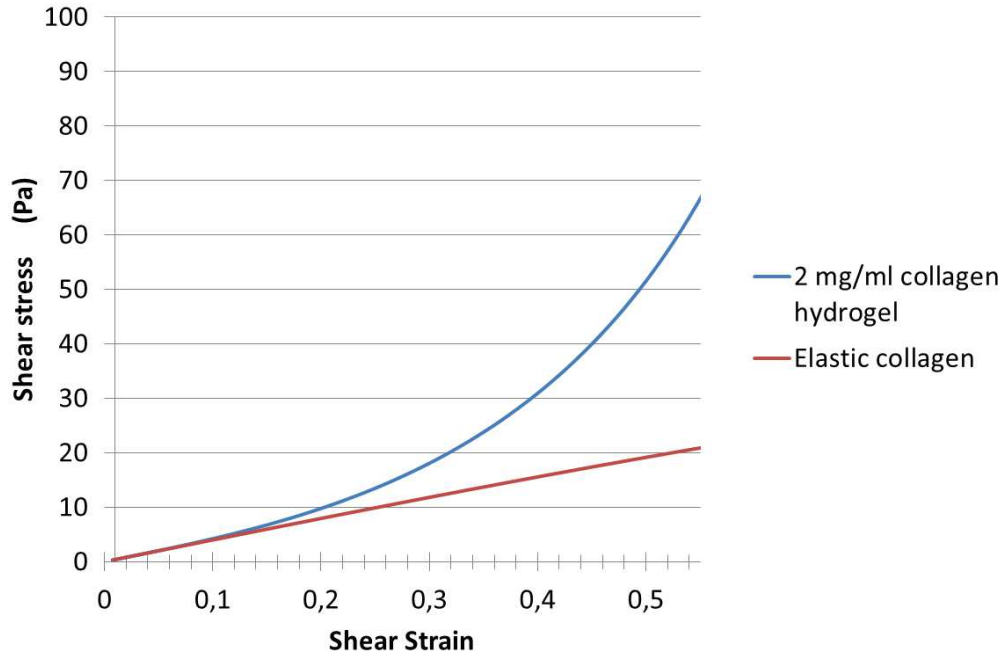


Figure 2.3: Shear stress versus shear strain (Appendix B) for 2 mg/ml collagen hydrogel and a linear elastic matrix with the same initial Young's modulus (elastic collagen).

To represent solid phase of collagen matrices, we use a hyperelastic constitutive model based on a uniform continuous fiber distribution [12]. This model captures the major features of the material properties of collagen gels, including non-linear elasticity, tension-compression non-linearity, and strain-dependent Poisson's ratio. To characterize the parameters from equation 2.2, we carried out a computational shear stress test (Appendix B) using experimental data [11]. This test simulates a ECM sample in a rheometer.

The strain energy function for the hyperelastic model used for collagen hydrogels is:

$$U = C \cdot (\hat{I}_1 - 3) + \frac{1}{D} \cdot \left(\frac{(J^{el})^2 - 1}{2} - \ln J^{el} \right) + \frac{k_1}{2 \cdot k_2} \cdot \sum_{\alpha=1}^N \left\{ \exp \left[k_2 \langle \bar{E}_\alpha \rangle^2 \right] - 1 \right\} \quad (2.2)$$

with

$$\bar{E}_\alpha = \kappa \cdot (\hat{I}_1 - 1) + (1 - 3 \cdot \kappa) \cdot (\hat{I}_{4(\alpha\alpha)} - 1) \quad (2.3)$$

where C , D , k_1 , k_2 and κ are material parameters, N is the number of families of fibers ($N \leq 3$), \hat{I}_1 is the first invariant of the right Cauchy-Green deformation tensor, J^{el} is the elastic volume ratio and $\hat{I}_{4(\alpha\alpha)}$ are pseudo-invariants of the right Cauchy-Green deformation tensor. Parameter κ is fixed 0.33 assuming the material isotropic.

To simulate the cell, several simplifications are made and only two parts are taken into account: nucleus and cytoplasm. The nucleus is considered a Neo-Hookean hyperelastic material with an equivalent Young's modulus and Poisson's ratio of 10 *kPa* and 0.49 respectively, in accordance with the work of Friedl et al. [13] and Vaziri et al. [14]. The strain energy function presents the following form:

$$U = C \cdot (\hat{I}_1 - 3) + \frac{1}{D} \cdot (J^{el} - 1)^2 \quad (2.4)$$

Finally, the cytoplasm is simulated as porous-elastic material. This is constituted by two distinct phases, the solid matrix (which is also modelled as a Neo-Hookean material) and the fluid flowing through solid matrix porous. On the solid phase, we assume a Young's modulus of 500 Pa and a Poisson's ratio of 0.3 ($C = 96.2 Pa$ and $D = 4.8 \cdot 10^{-3} Pa$ constants for Neo-Hookean equation), but also a case with 0.4 is simulated. To define the fluid phase, we use the permeability of the solid phase (wherein is implicit the viscosity of the fluid [15]), the void ratio and the specific weight. We chose values of

	Cytoplasm
Young's modulus of solid phase	500 Pa
Poisson's ratio of solid phase	0.3
Permeability of fluid	$4 \cdot 10^{-20} \frac{m^4}{N \cdot s}$

Table 2.3: Mechanical properties of cytoplasm.

cytoplasm stiffness and permeability that are compatible with previous studies [16, 17]. We also perform a finite element model to study the relationship between the Young's modulus for a elastic material and for the solid phase of a porous-elastic material (Appendix A). Since the fluid phase increases the apparent stiffness on the transitory analysis, we decrease the elastic modulus of the solid phase of the cytoplasm. The permeability is reduced 5 orders of magnitude to reproduce the pressures measured into the cytoplasm by Petrie et al., [7]. All mechanical properties of cytoplasm are shown in the Table 2.3.

Furthermore, we perform another model in which the cytoplasm is simulated as fluid, using the fluid-structure interaction (FSI) calculation scheme. Nonetheless, FSI model is discarded because of the quasi-static movement of the nucleus.

2.3 Boundary and loading conditions

As a initial conditions, we fix all displacement of the ECM external surface, we assume zero pressure inside the cytoplasm and we also fix the flow rate through the interface cell-matrix to avoid lost of fluid in the cytoplasm.

In addition, we apply pressure on the back surface of the nucleus to simulate core movement (Figure 2.4a). We increase this pressure from 0 to 400 Pa in the first 50 seconds and it remained constant in the last 50 seconds (Figure 2.4b). The total time simulated is 100 seconds.

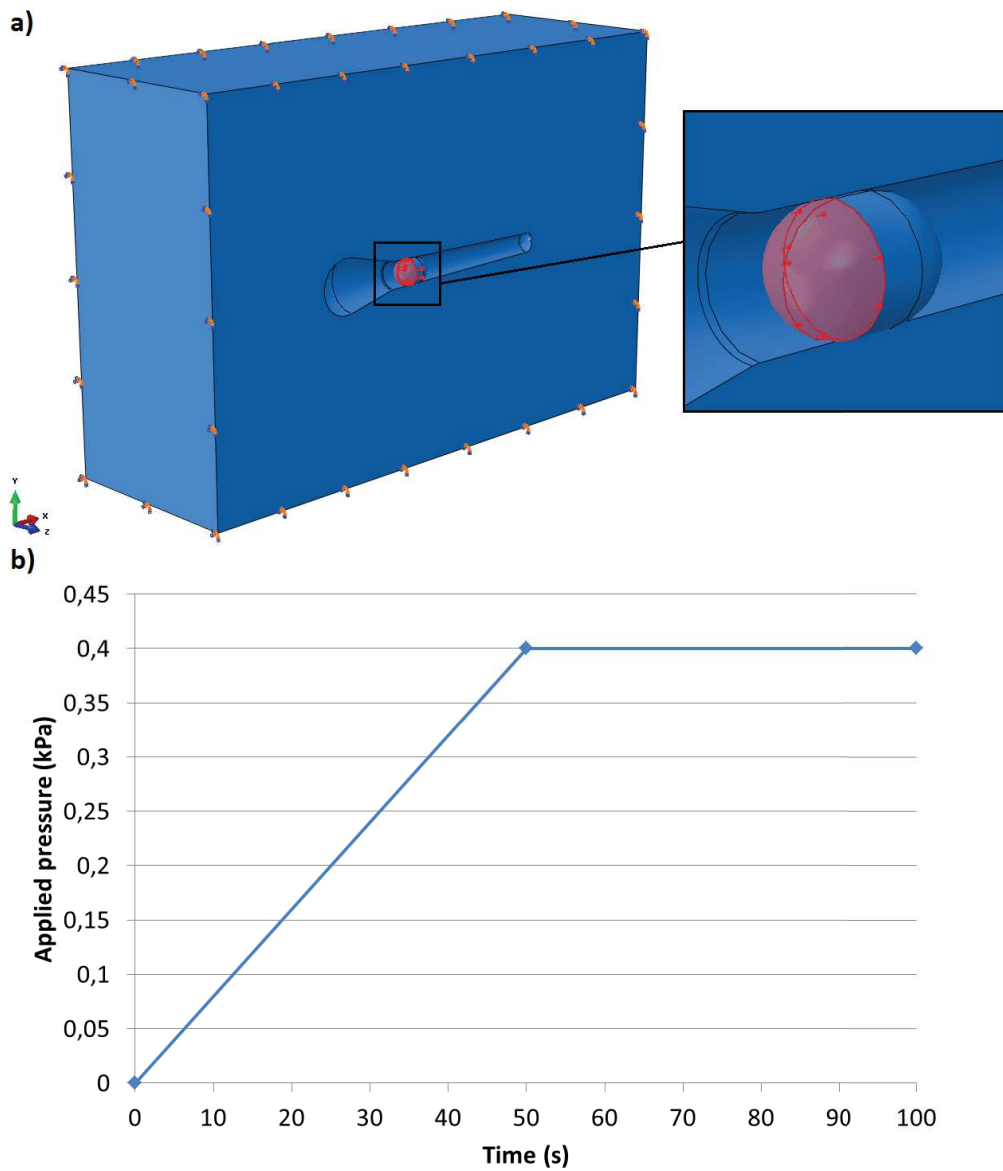


Figure 2.4: Description of boundary conditions and pressure application (a) and instant pressure applied (b).

Chapter 3

Results and discussion

We focus our analysis of the simulation results on the advance of the nucleus inside of the lobopodio, the generation of a pressure gradient between the front and back part of the nucleus, the stresses on the cell nucleus and the ECM strains. All measurements are taken at time 50 seconds, when the pressure applied is 400 Pa .

3.1 Nucleus displacement through lobopodio

First, we analyse the displacement of the back edge of the nucleus (Figure 3.1). The displacement depends on the capability of the nucleus to deform the cytoplasm and the surrounding matrix. Figure 3.2 shows the displacement along time for all the matrices studied. As expected, nucleus displacement is larger on softer matrices in the case of linear elastic matrices (elastic collagen, CDM and dermal explant). For all simulations, the nucleus deformation is not taken into account (less than 3%).

To study the influence of the matrix Poisson's ratio, one case is computed with the CDM matrix but varying ν_{ECM} to 0,3. The results obtained from the CDM matrix with 0,48 and 0,3 Poisson's ratio show that the nucleus displacements and velocity increase for higher compressibility (Figure 3.2). Thus, the Poisson's ratio of the matrix is relevant for lower elastic modulus or higher velocities, in other case it is not an important parameter for which is needed good accuracy.

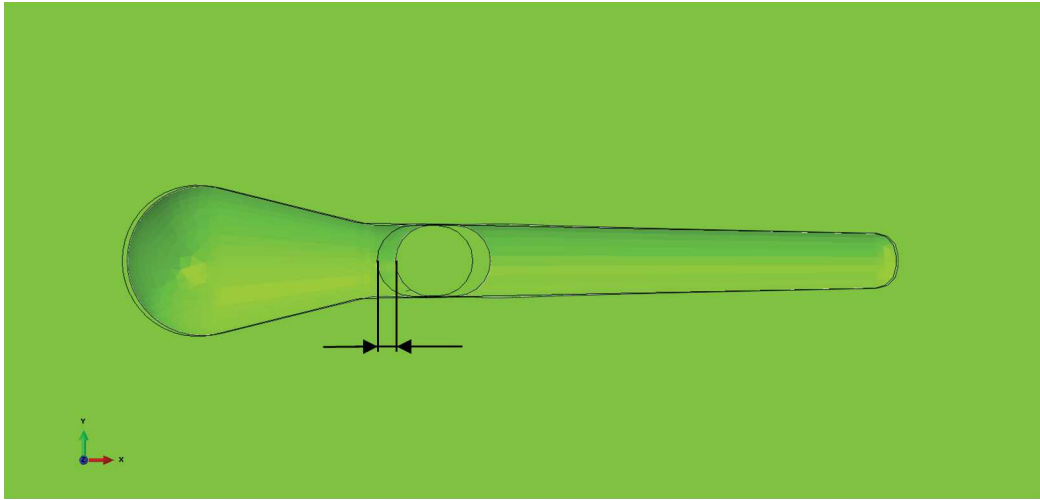


Figure 3.1: Scheme of trailing edge displacement.

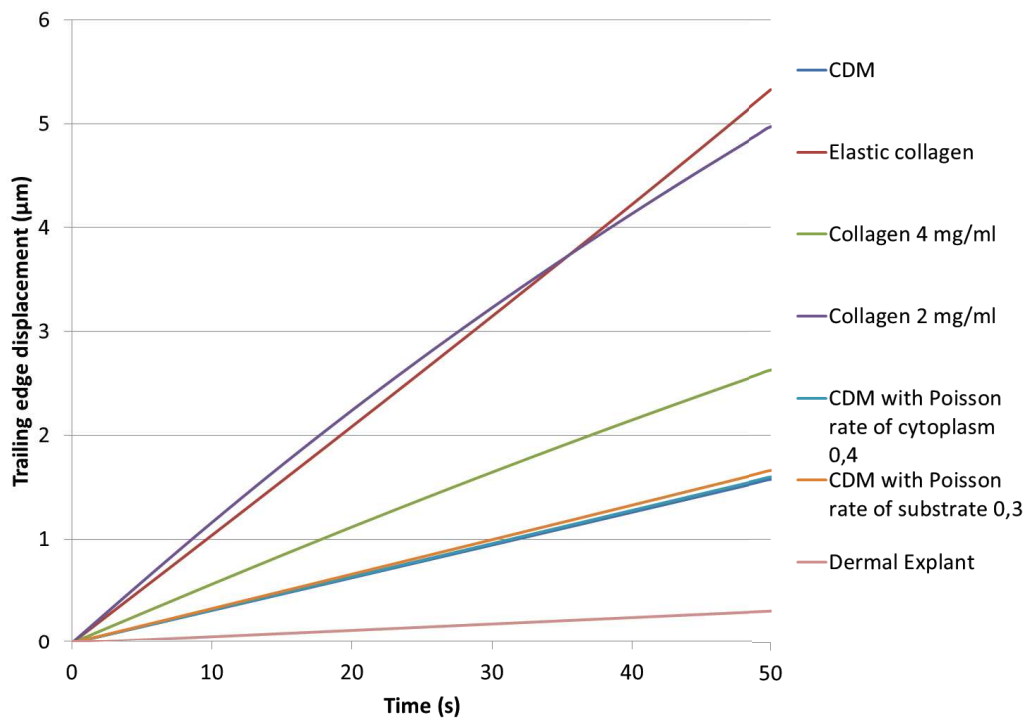


Figure 3.2: Trailing edge displacements.

Moreover, we simulate a case with 0,3 Poisson's ratio for the cytoplasm instead of 0,4 and we do not observe any changes on our results.

Regarding the results from linear and non-linear elastic matrices, we observe different behaviour. On collagen hydrogels, the nucleus velocity is not constant and its decreases with time due to the strain stiffening. Nevertheless, the velocity of the nucleus is constant on elastic matrices. We can see this difference in Figure 3.2, comparing the velocities of nucleus in 2 mg/ml collagen hydrogel and elastic collagen matrices. For elastic collagen matrix the velocity is constant, but for 2 mg/ml collagen hydrogel it starts with a higher velocity and decreases until being lower.

The velocities obtained for the pressure values applied on the nucleus are in the order of $10^{-2}\mu m/s$. These results are compatible with the measurements obtained experimentally by Petrie et al. [7] for the CDM matrix.

3.2 Hydrostatic pressure in the cytoplasm

Petrie et al. [7] measured the intracellular hydrostatic pressure in the front and back part of the nucleus obtaining values of 2400 Pa and 900 Pa respectively for the CDM matrix. On cell migration, there are several phenomena that can increase the internal pressure in the cell, such as actomyosin contractility. However, the pressure gradient between the front compartment and the back compartment of the cell is mainly caused by the nucleus movement. Nonetheless, our computational model simulates the nucleus movements but it does not take into account other cell mechanism. So that, the pressure gradient has been measured instead of absolute pressure values.

Figures 3.3 and 3.4 show hydrostatic pressure of the fluid for the linear elastic and strain-dependent matrices respectively. The pressure gradient is higher on the case in which nucleus displacement is larger. The value of the pressure gradient is close to 850 Pa for the elastic collagen and 2 mg/ml collagen hydrogel matrices. In addition, the absolute values of pressure are similar in the front and back part of the nucleus. Thus, the gradient pressure is similar on the simulations with linear elastic and strain-dependent matrices. With respect to the effect of Poisson's ratios of the CDM matrix and solid phase of the cytoplasm, there are not differences in the hydrostatic pressure. Finally, the gradient pressure for dermal explant matrix is the lower of all cases and it is close to 320 Pa.

Therefore, there are not differences in the hydrostatic gradient depending if the matrix is elastic or strain-dependent, but there are with the displacement and the velocity.

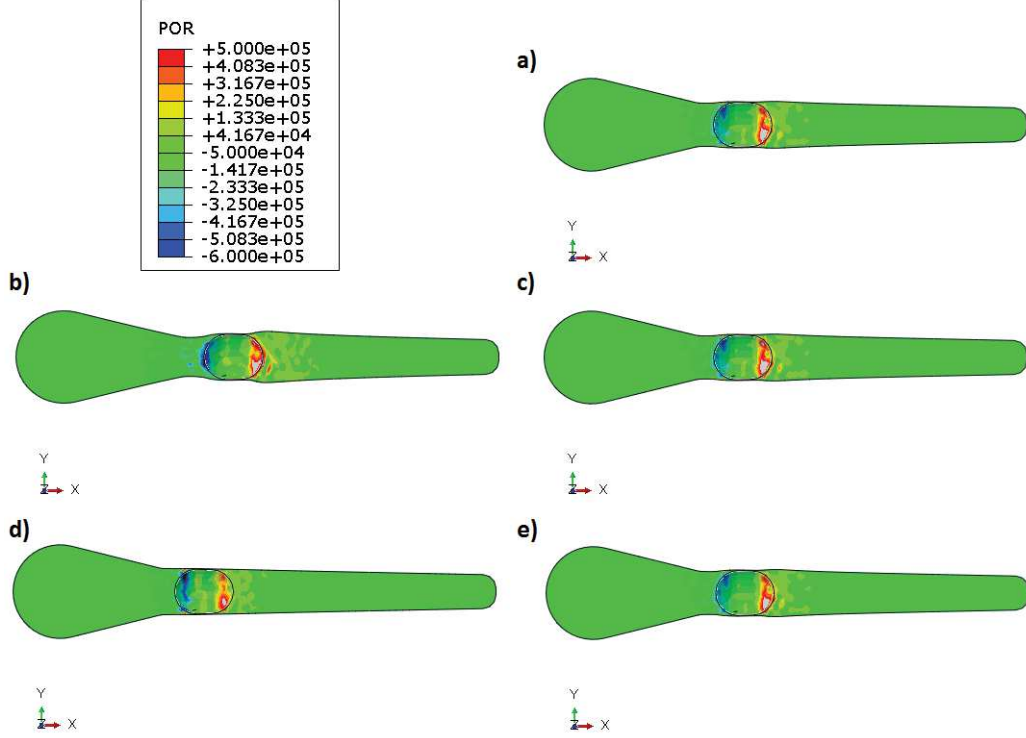


Figure 3.3: Hydrostatic pressure in the cytoplasm; a) CDM matrix, b) elastic collagen, c) CDM with $\nu_{cytoplasm} = 0,4$, d) dermal explant, e) CDM with $\nu_{ECM} = 0,3$ (units mPa).

In spite of all results are taken at the end of the transient state, because of the we are interesting in the transient response of the system, we also simulate 50 seconds with a constant pressure applied. In this time, the fluid part of the cytoplasm starts to relax and the pressure decreases.

3.3 Strains of the matrix

Other result analysed is the matrix strains on our model. For all cases simulated, the pressure applied to the nucleus is the same, thereby the main factor regulating the cell deformation is the matrix. In Figures 3.5 and 3.6

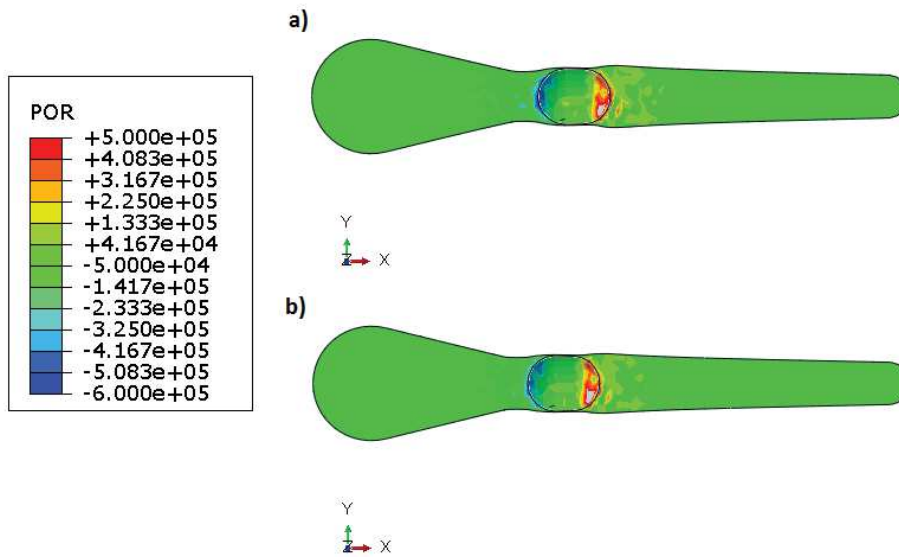


Figure 3.4: Hydrostatic pressure in the cytoplasm; a) 2 mg/ml collagen hydrogel, b) 4 mg/ml collagen hydrogel (units mPa).

we can observe the strains on linear elastic and strain-dependent matrices respectively. For a dermal explant matrix (Figure 3.5d) there is almost no matrix deformation due to its high elastic modulus. However, the elastic collagen (Figure 3.5b) shows strains of 60 % (and very close to the nucleus). For CDM matrices, matrix strain distribution is similar to elastic collagen but with lower values. In addition, the Poisson's ratios of matrix and cytoplasm solid phase are not relevant for the results. In all CDM cases, matrix strains are under 20 %.

Regarding strain-dependent matrices (Figure 3.6), the strain distribution is different from linear elastic matrices. They show lower matrix strains due to the stiffening. Strains are more distributed on the matrix and the maximum value is 40 % for 2 mg/ml collagen matrix instead of 60 % for elastic collagen matrix (comparison of Figures 3.5b and 3.6a).

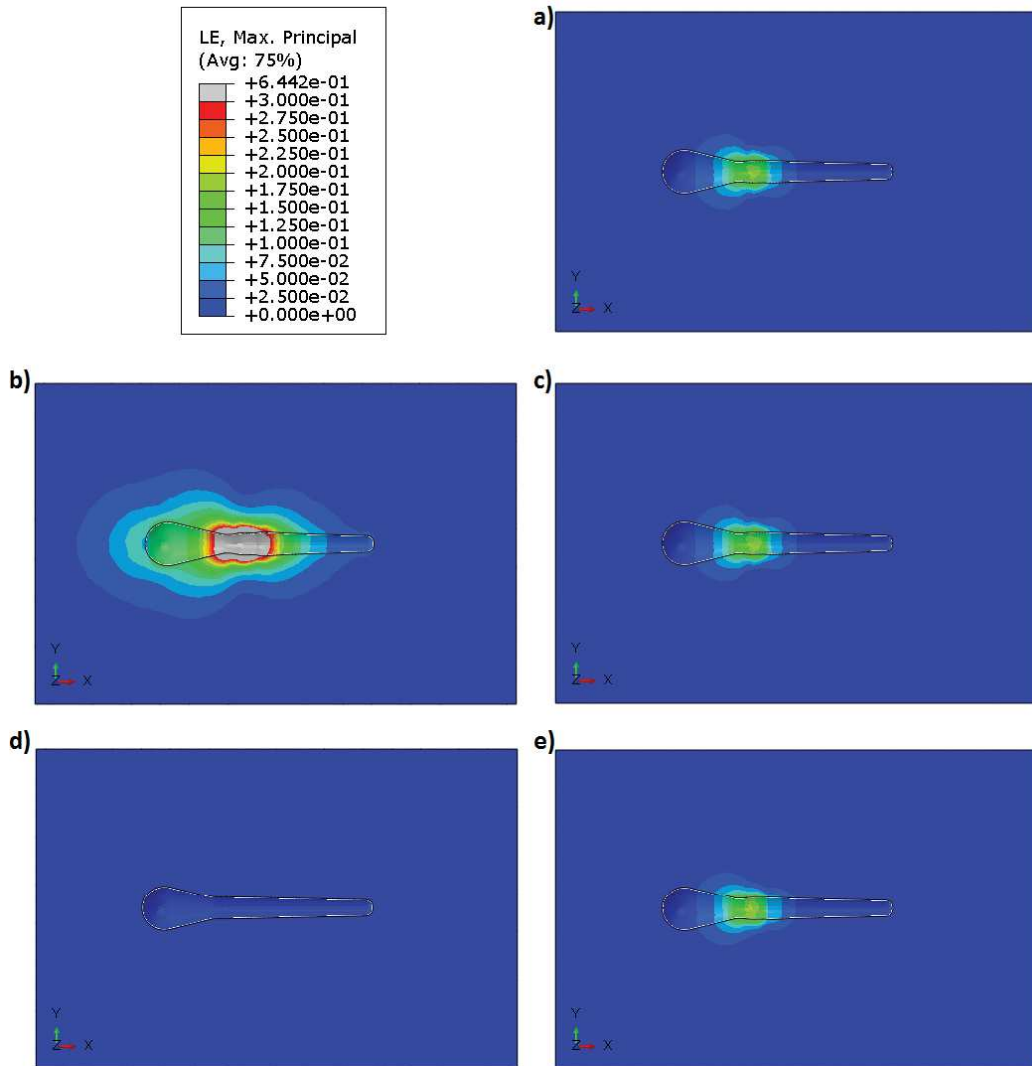


Figure 3.5: Strain on the ECM; a) CDM matrix, b) elastic collagen, c) CDM with $\nu_{cytoplasm} = 0,4$, d) dermal explant, e) CDM with $\nu_{ECM} = 0,3$.

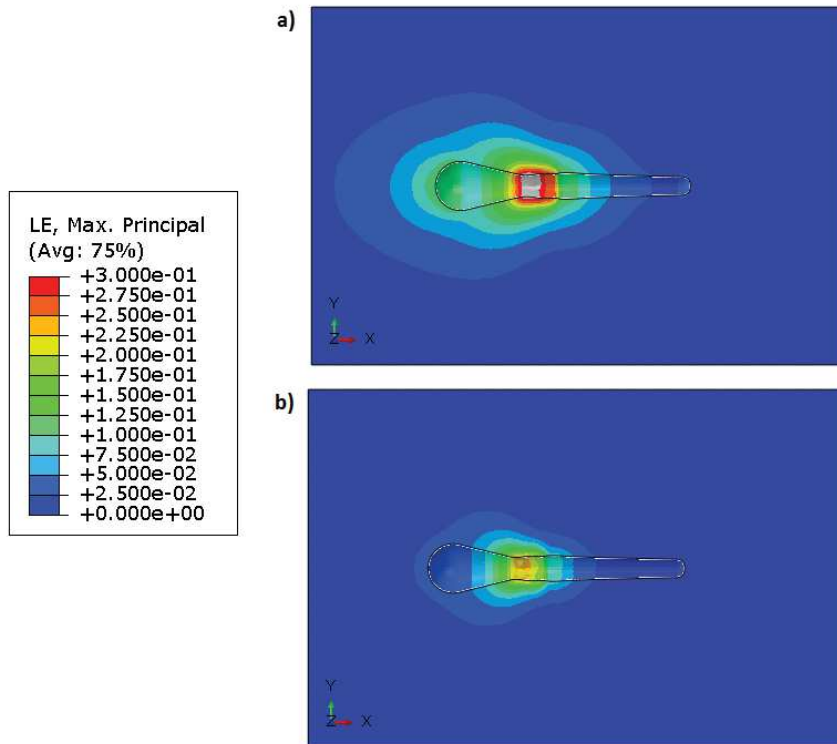


Figure 3.6: Strain on the ECM; a) 2 mg/ml collagen hydrogel, b) 4 mg/ml collagen hydrogel (units mPa).

3.4 Nucleus stress

Finally, we analyse the mechanical state of the nucleus. We obtain the maximum tensile stress (Figures 3.7 and 3.8) and the maximum compressive stress (Figures 3.9 and 3.10) of the cell nucleus.

In all simulations, the cell nucleus is mainly under compression because of we are pushing forward it. Figures 3.7 and 3.8 show similar distribution of tensile stress, for all cases except for dermal explant matrix which is all under compression. The others six cases simulated show a focus area in the leading edge in which appears tensile stresses of 25 Pa.

Regarding the maximum compression stress, we observe also a similar distribution in all cases. The front part of the nucleus show lower stress, possibly because of the surrounding material (cytoplasm) have lower Young's

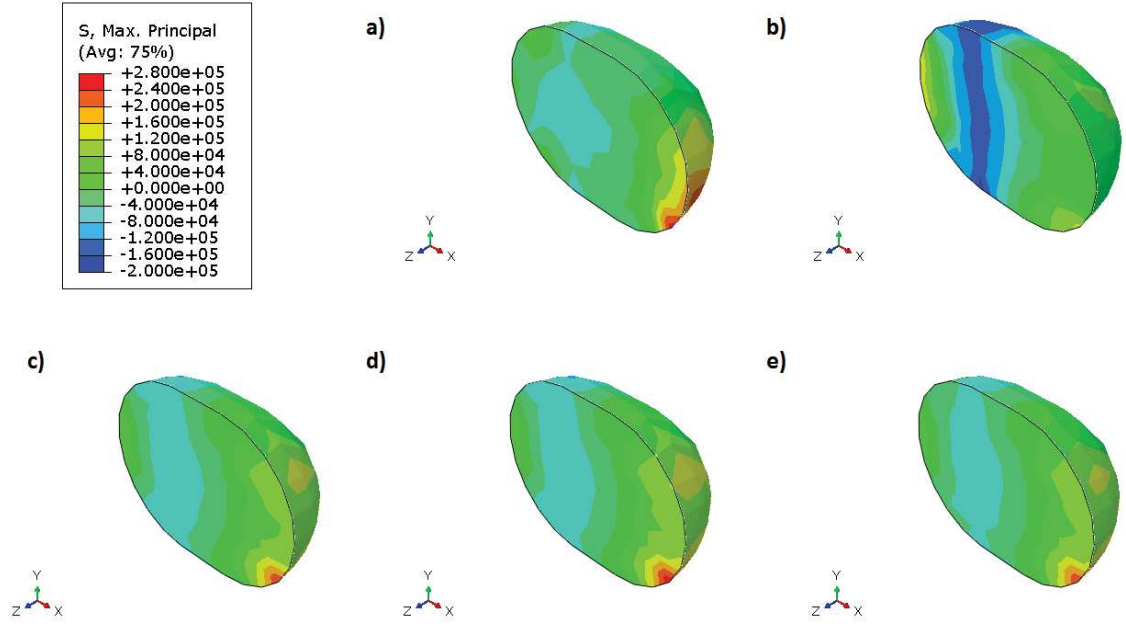


Figure 3.7: Maximum tensile stress on the nucleus; a) elastic collagen matrix, b) dermal explant matrix, c) CDM matrix, d) CDM matrix with $\nu_{cytoplasm} = 0,4$, e) CDM matrix with $\nu_{ECM} = 0,3$ (units mPa).

modulus. However, the highest compression stresses appears on the interface between the surface where we apply the pressure and the surface where we do not apply it. Thus, this maximum values may be erroneous due to our boundary conditions.

Therefore, we do not observe differences between linear elastic and strain-dependent matrices on the nucleus stress, neither between the variants of CDM matrix. However, we observe that the elastic modulus of the matrix has effect on the values of the stresses. The higher the Young's modulus, the higher the compression stresses.

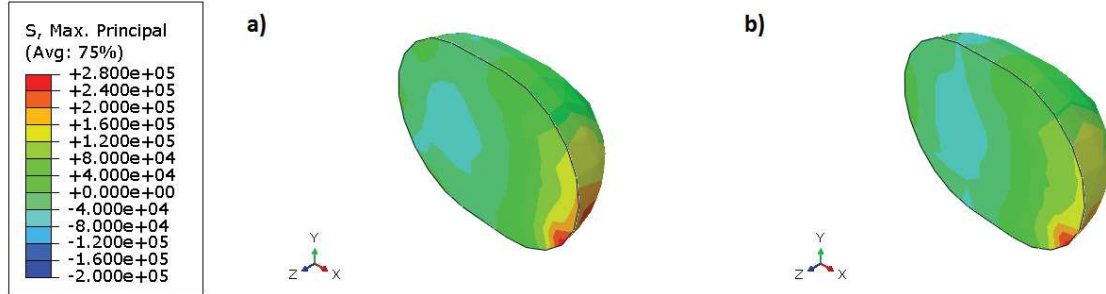


Figure 3.8: Maximum tensile stress on the nucleus; a) 2 mg/ml collagen hydrogel, b) 4 mg/ml collagen hydrogel (units mPa).

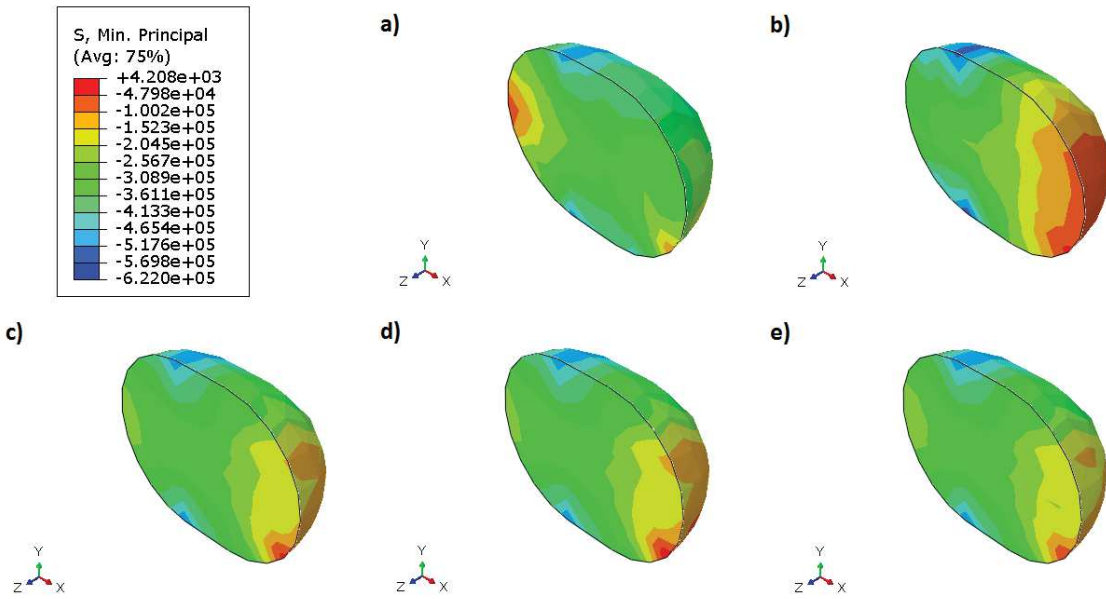


Figure 3.9: Maximum compression stress on the nucleus; a) elastic collagen matrix, b) dermal explant matrix, c) CDM matrix, d) CDM matrix with $\nu_{cytoplasm} = 0,4$, e) CDM matrix with $\nu_{ECM} = 0,3$ (units mPa).

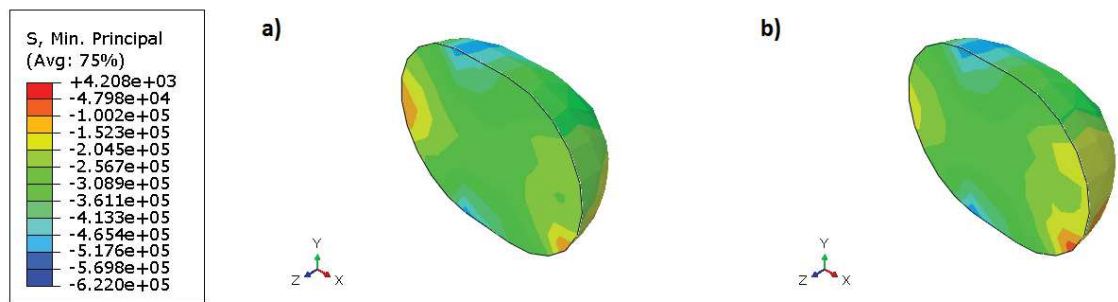


Figure 3.10: Maximum compression stress on the nucleus; a) 2 mg/ml collagen hydrogel, b) 4 mg/ml collagen hydrogel (units mPa).

Chapter 4

Conclusion

In this Master's Thesis, we develop a finite element model of lobopodial-based migration in different linear and non-linear matrices. We consider the surrounding matrix as linear elastic and strain-dependent materials, the cytoplasm as porous-elastic and the nucleus as Neo-Hookean material.

One of the main difficulties we found to properly model and simulate cell migration is to accurately characterise the cytoplasm mechanical properties. Cytoplasm is a very heterogeneous part of the cell and it is composed by a large number of organelles through which flows the cytosol. Hence, we consider the cytoplasm as a homogeneous porous elastic material. Nevertheless, measuring the properties of fluid and solid phase is a difficult task. Thus, considering the instantaneous response of the cytoplasm, we do not use exactly the same permeability value shown on Taber et al.[16] and it is only taken as a reference value. The value of elastic modulus of the solid phase is approximated using an additional finite element model and the experimental data by Efremov et al. [17].

Otherwise, one of the main objectives of this study is to elucidate if linear and non-linear elastic matrices affect the lobopodia-based migration. To compare directly both matrices, the elastic collagen has the same properties initially as 2 mg/ml collagen hydrogel, however, collagen becomes stiffer with the strain. The work of Petrie et al. [5] conclude with a three-question path to know what type of cell migration is going to appear; what is the dimensionality of the matrix, what is the level of RhoA activity, and is the 3D matrix linearly elastic? For strain-dependent matrices they find that cells will choose lamellipodia.

Thereby, we analyse hydrostatic pressure inside the cytoplasm, nucleus stresses, matrix strains and nucleus displacement as main results.

The hydrostatic pressure gradient between the leading and trailing edge of the nucleus was compatible with experimental work of Petrie et al. (2014) [7] for the force applied. Nevertheless, we do not find large differences between linear and non-linear matrices, but between the different linear matrices depending on the elastic modulus.

For the stress on the nucleus, we only observe differences in the elastic modulus of the matrix. This is a normal result because with higher stiffness, the nucleus find more resistance to advance.

Analysing the matrix strains, we observed different distributions for linear and non-linear matrices due to in the local zones where the strain is higher the stiffness increases. And, as expected, strains are higher on softer matrices because of the nucleus displacement is larger. But again, we do not find significantly differences between linear and non-linear matrices.

Finally, nucleus displacements and velocities are also compatible with experimental works [7] for CDM matrix. Regarding the differences between linear and non-linear elastic behaviour, we observe the stiffening of the matrix with a decrease of the nucleus velocity. In spite of this, the nucleus advances more in a 2 mg/ml collagen hydrogel than in a CDM linear matrix.

Thus, we have not found a mechanical explanation for the preference of cells to use lamellipodia-based migration instead of lobopodia-based for strain-dependent matrices. First, we can think that the stiffening causes the cell to change from lobopodia- to lamellipodia-based cell migration. However, the simulation of matrices with different behaviours show how there are not evidences of this hypothesis. The gradient pressure generated by the nucleus is very similar for a cell in collagen hydrogel of 2 *mg/ml* and in elastic collagen matrix. The stresses suffer by the nucleus are also very similar for linear elastic and strain-dependent material, it depend with the stiffer of the matrix but not with the behaviour. And finally, despite of there are differences in the matrix strain distribution, the nucleus in a 2 mg/ml collagen hydrogel advances more than in a CDM matrix, which is no strain-dependent but it have a higher elastic modulus.

4.1 Future work

In a future work, it is possible to extend this model adding actomyosin contraction behaviour of cell in order to obtain the real hydrostatic pressures instead of a gradient. Furthermore, it may reveal an explication about why exist this difference between linear and non-linear matrix behaviour that only with the nucleus movement we cannot observe. In addition, it is also possible add membrane cell or organelles, contributing stiffness to cell and heterogeneity to the cytoplasm respectively.

Moreover, it may be interesting to study the influence of the nucleus properties. There are studies where the nucleus Poisson's ratio take negative values [18] or becomes stiffer due to the effect of drugs [19]. Both parameters may be important in cell migration.

Bibliography

- [1] M. H. Zaman, L. M. Trapani, A. L. Sieminski, D. MacKellar, H. Gong, R. D. Kamm, A. Wells, D. A. Lauffenburger, P. Matsudaira, Migration of tumor cells in 3d matrices is governed by matrix stiffness along with cell-matrix adhesion and proteolysis, *Proceedings of the National Academy of Sciences* 103 (29) (2006) 10889–10894.
- [2] P. Friedl, K. Wolf, Plasticity of cell migration: a multiscale tuning model, *The Journal of Cell Biology* 188 (1) (2010) 11–19. arXiv:<http://jcb.rupress.org/content/188/1/11.full.pdf>, doi:10.1083/jcb.200909003.
URL <http://jcb.rupress.org/content/188/1/11>
- [3] T. Luque, E. Melo, E. Garreta, J. Cortiella, J. Nichols, R. Farré, D. Navajas, Local micromechanical properties of decellularized lung scaffolds measured with atomic force microscopy, *Acta Biomaterialia* 9 (6) (2013) 6852 – 6859. doi:<http://dx.doi.org/10.1016/j.actbio.2013.02.044>.
URL <http://www.sciencedirect.com/science/article/pii/S1742706113001141>
- [4] A. J. Ridley, M. A. Schwartz, K. Burridge, R. A. Firtel, M. H. Ginsberg, G. Borisy, J. T. Parsons, A. R. Horwitz, Cell migration: integrating signals from front to back, *Science* 302 (5651) (2003) 1704–1709.
- [5] R. J. Petrie, N. Gavara, R. S. Chadwick, K. M. Yamada, Nonpolarized signaling reveals two distinct modes of 3d cell migration, *The Journal of Cell Biology* 197 (3) (2012) 439–455. arXiv:<http://jcb.rupress.org/content/197/3/439.full.pdf>, doi:10.1083/jcb.201201124.
URL <http://jcb.rupress.org/content/197/3/439>
- [6] D. W. DeSimone, A. R. Horwitz, Many modes of motility, *science* 345 (6200) (2014) 1002–1003.

- [7] R. J. Petrie, H. Koo, K. M. Yamada, Generation of compartmentalized pressure by a nuclear piston governs cell motility in a 3d matrix, *Science* 345 (6200) (2014) 1062–1065.
- [8] R. J. Petrie, K. M. Yamada, Multiple mechanisms of 3d migration: the origins of plasticity, *Current Opinion in Cell Biology* 42 (2016) 7 – 12, cell dynamics. doi:<https://doi.org/10.1016/j.ceb.2016.03.025>.
URL <http://www.sciencedirect.com/science/article/pii/S0955067416300758>
- [9] O. Moreno-Arotzena, C. Borau, N. Movilla, M. Vicente-Manzanares, J. M. García-Aznar, Fibroblast migration in 3d is controlled by haptotaxis in a non-muscle myosin ii-dependent manner, *Annals of Biomedical Engineering* 43 (12) (2015) 3025–3039. doi:10.1007/s10439-015-1343-2.
URL <http://dx.doi.org/10.1007/s10439-015-1343-2>
- [10] K. E. Kubow, S. K. Conrad, A. R. Horwitz, Matrix microarchitecture and myosin {II} determine adhesion in 3d matrices, *Current Biology* 23 (17) (2013) 1607 – 1619. doi:<https://doi.org/10.1016/j.cub.2013.06.053>.
URL <http://www.sciencedirect.com/science/article/pii/S0960982213007781>
- [11] C. Valero, H. Amaveda, M. Mora, J. M. García-Aznar, Mechanical characterization of cross-linked collagen-based hydrogels, Under review.
- [12] T. C. Gasser, R. W. Ogden, G. A. Holzapfel, Hyperelastic modelling of arterial layers with distributed collagen fibre orientations, *Journal of the royal society interface* 3 (6) (2006) 15–35.
- [13] P. Friedl, K. Wolf, J. Lammerding, Nuclear mechanics during cell migration, *Current Opinion in Cell Biology* 23 (1) (2011) 55 – 64, cell structure and dynamics. doi:<http://dx.doi.org/10.1016/j.ceb.2010.10.015>.
URL <http://www.sciencedirect.com/science/article/pii/S0955067410001869>
- [14] A. Vaziri, H. Lee, M. K. Mofrad, Deformation of the cell nucleus under indentation: mechanics and mechanisms, *Journal of materials research* 21 (08) (2006) 2126–2135.
- [15] E. Moeendarbary, L. Valon, M. Fritzsche, A. R. Harris, D. A. Moulding, A. J. Thrasher, E. Stride, L. Mahadevan, G. T. Charras, The cytoplasm of living cells behaves as a poroelastic material, *Nature materials* 12 (3) (2013) 253–261.
- [16] L. Taber, Y. Shi, L. Yang, P. Bayly, A poroelastic model for cell crawling including mechanical coupling between cytoskeletal contraction and

- actin polymerization, *Journal of mechanics of materials and structures* 6 (1) (2011) 569–589.
- [17] Y. Efremov, M. Lomakina, D. Bagrov, P. Makhnovskiy, A. Alexandrova, M. Kirpichnikov, K. Shaitan, Mechanical properties of fibroblasts depend on level of cancer transformation, *Biochimica et Biophysica Acta (BBA) - Molecular Cell Research* 1843 (5) (2014) 1013 – 1019. doi:<http://dx.doi.org/10.1016/j.bbamcr.2014.01.032>. URL <http://www.sciencedirect.com/science/article/pii/S0167488914000445>
- [18] S. Pagliara, K. Franze, C. R. McClain, G. W. Wylde, C. L. Fisher, R. J. M. Franklin, A. J. Kabla, U. F. Keyser, K. J. Chalut, Auxetic nuclei in embryonic stem cells exiting pluripotency, *Nature Materials* 13 (6) (2014) 638–644. doi:10.1038/nmat3943.
- [19] B. Zhang, Q. Luo, Z. Chen, Y. Shi, Y. Ju, L. Yang, G. Song, Increased nuclear stiffness via fak-erk1/2 signaling is necessary for synthetic mechano-growth factor e peptide-induced tenocyte migration, *Scientific reports* 6.